Spot-Probe Reflectometer Measurements of Geological Core Slab Samples

Jose Oliverio Alvarez
Sensors Development
Aramco Services Company – Aramco Research Center
Houston, TX, USA
Oliverio.alvarez@aramcoservices.com

John W. Schultz
Compass Technology Group
Alpharetta, GA, USA
John.Schultz@compasstech.com

Abstract— **Rock core specimens collected during surveys for oil drilling have, in a standard form, a 4" diameter. Cores are cut in half or in 1/3-2/3 sections to provide core slab. We developed a measurement procedure based on spot probe illumination to characterize geological and/or geochemical properties of core slab specimens via their complex permittivity for frequencies between 2.5 GHz and 20 GHz. Conventional reflectometer methods are based on illumination of a thin slab of air- or metal-backed material. However, in this case only the front surface is flat and the back surface is semicircular. A measurement method was developed based on time-domain gating to separate the back-surface reflection from that of the front. Material inversion is then based on the amplitude and phase of the reflection just from the front surface. This paper presents details of the calibration for this reflectometer measurement method, along with example measurements of core slab materials. Two different inversion methods are applied to these measured data. The first is a more conventional frequency-by-frequency method for inverting complex permittivity from the amplitude and phase of the reflection. The second method applies a physical model, the Debye relaxation model, to the data. This model-based approach minimizes the errors from edge diffraction from the small sample size.**

I. Introduction

In the petroleum industry there are two broad classes of measurements performed in a well: indirect and direct measurements. Indirect measurements are carried out with downhole logging tools using different methods to characterize specific properties of the rock and the fluids contained in it. Indirect measurements are limited by having to be applied in the well environment, which restricts the size and complexity of the measurement sensor and method. Conversely, direct measurements consist of extracting rock core samples and performing the measurements directly in the relatively undisturbed formation. Direct measurements have the disadvantage of being not-immediate since specimens are first extracted and then characterized in a laboratory later. However, the advantage of the direct measurements is that a richer set of information can be gleaned about the rock since the laboratory environment accommodates a wider range of measurement apparatus.

Coring takes place between drilling operations and if handled correctly, rock cores provide the most complete ground truth measurements. This ground truth is then used to calibrate and integrate all other (indirect or seismic) measurements. Typically, a large diameter core (3" to 5.25" diameter) is extracted and cut into 1-meter sections. These sections are then slabbed into either 1/3-2/3 sections or in two halves. Smaller core plugs (1" to 1.5" diameter) are taken to perform different measurements (e.g. grain size, porosity, permeability and water saturation). **Error! Reference source not found.**[2]

Depending on the availability of a coring laboratory, a routine core analysis can take anywhere from two weeks to a few months. Moreover, due to complicating logistical factors, it is estimated that a large percentage of the current core analysis data are unfit for many purposes due to their unreliability and inapplicability. Therefore, there is a strong need in the drilling industry for new and more robust characterization methods such as presented here.

This study presents a nondestructive electromagnetic measurement procedure for geological core slabs. This method is a new alternative to conventional core analysis techniques. The method is based on microwave spot probe illumination and computes the complex permittivity from 2.5 GHz to 20 GHz from the measured reflection or S_{11} data. These measurements, when compared with core analysis data, can be used to characterize geochemical properties of the rock. The results may then enable the design of an electromagnetic diagnostic logging tool that can identify geological/geochemical features.

II. Spot Probe Fixture & Methodology

The use of dielectrically loaded spot probes for microwave materials measurements has been around for several decades. [3] The probe antenna forms a beam that roughly approximates a plane wave, which then interacts with a material specimen. To minimize fixture size, the spot probe is designed to illuminate a specimen either adjacent to it or in close proximity. In this research, we employed wide-band spot probes developed several years ago to have enhanced bandwidth over previous generation spot probes [1]. The spot probe used in the present work includes both metallic elements and dielectric material integrated into a compact and rugged design that has excellent performance.

The probe is shaped to form an approximately symmetrical illumination spot a few centimeters in front of the end. The 'focus' of the beam is at the probe tip and the beam diameter

therefore grows with distance from the probe tip. At 2.5 cm (1 inch) from the probe tip the beam diameter is approximately 3 cm (1.2 inches). At 7.6 cm (3 inches) from the probe tip, the beam diameter is approximately 6.3 cm (2.5 inches). Note that these dimensions are in the middle of the operating band (near 10 GHz). Because the probe has a fixed physical aperture, the beam width decreases with frequency. So it is a larger illumination spot at low frequency and a smaller spot at high frequencies.

A photograph of the spot probe measuring a slab specimen is shown in Figure 1. The spot probe is mounted on a tripod stand and is pointing up. Mounted on the end of the spot probe is a spacer manufactured from a 3-D printed hard rubber and shaped into a low-dielectric honeycomb structure. This spacer maintains a constant distance between the active end of the probe and the specimen under test. The photograph in this Figure also shows a typical rock slab specimen resting on top of the low-dielectric spacer. The rock slab is a semi cylindrical shape that was cut from a cylinder core sample. If desired, additional fixturing may be used to enable scanning of a core slab to determine material homogeneity.

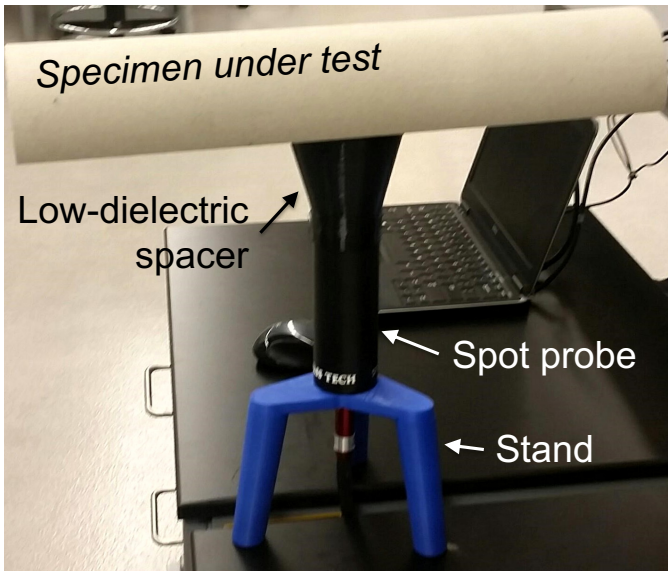

Figure 1 Photograph of spot probe fixture measuring a rock specimen.

For reflection measurements, the calibration procedure uses a "response and isolation" method. The Response calibration, standard is a flat metal plate, while the isolation standard is a measurement of free space or no sample. In this method the isolation standard is vector-subtracted from the response standard as well as from the specimen measurement to minimize the effects of mismatch reflections in the probe and network analyzer port. The calibrated S_{11} is calculated from,

$$S_{11}^{cal} = \frac{S_{11}^{measured} - S_{11}^{isolation}}{S_{11}^{response} - S_{11}^{isolation}} \quad (1)$$

The response standard also provides a phase reference measurement. To have accurate phase information about the specimen, the measured surface of the metal reference must be in the same place as the front surface of the specimen under test. This is why the low dielectric spacer is used in the fixture, so that this phase reference distance is maintained, as shown in Figure 1.

To further improve measurement accuracy, a Fourier transform is applied to convert frequency-domain data into time-domain data. This enables the separation of the received signals into different components, namely i) the unknown specimen and ii) other discontinuities within the measurement system. Data measured with a network analyzer is discrete in frequency so a discrete transform is required to view the data in the time domain. The resolution in the time domain is proportional to the bandwidth of the frequency domain. The unambiguous range of the time domain is proportional to the number of points in the frequency domain. Therefore, using a high number of points over the full 2-20 GHz bandwidth of the probe is preferred so that the unambiguous range is large enough to avoid aliasing (overlap) with other undesired signals and so that other multipath effects can be separated from the desired reflection.

In time domain a gate is used to select only the signal of interest and subtract the undesired reflections outside of that gate. For this system the gate width is typically 0.5 nanoseconds or less, which corresponds to approximately 3 inches (7.5 cm) in free space. For the typical dielectric properties of the rocks under test, this corresponds to less than 2 inches (5 cm) within the material specimen.

This gating brings us to another important feature of the method described here. In most free-space material measurement techniques, a slab of finite thickness is measured, and both the front and back reflections contribute to the measured or transmitted signal. With the two-inch thick specimens as shown in Figure 1, the gate prevents the reflection from the back side of the sample to be measured, so that only the front surface reflection is captured. This is an important feature of the method since the back surface is curved. While the transmission-line theory used to invert material properties is very simple for planar interfaces, a curved surface complicates the inversion. In this method the curved surface interface is purposely ignored, keeping the inversion equations tractable.

III. Inversion Methods

Since the method's gating procedure removes the back-side reflection from the measured signal, the inversion is based only on the reflection from the front, flat-side of the slab. The assumption is that the material under test is homogeneous and that is looks like a semi-infinite half-space of material to the probe. For dielectric materials, the system collects amplitude and phase of the reflection coefficient, so at each frequency the complex dielectric permittivity, ε, can be solved for from the Fresnel reflection coefficient,

$$S_{11} = -\frac{1-\sqrt{\varepsilon}}{1+\sqrt{\varepsilon}} \quad (2)$$

One of the limitations of this measurement method is the small, approximately 4" diameter of the specimens. Specifically, in the 4" direction there is some interaction of the illumination

beam with the edge of the specimen. This results in edge diffraction which is also picked up by the spot probe. After inversion, this edge diffraction exhibits a frequency ripple across the measurement band. Example inverted dielectric properties for an alumina/silicate ceramic specimen are shown in Figure 2. The top plot is the real permittivity and the bottom plot shows the imaginary permittivity or loss. The blue curves in each of these plots are calculated with the above inversion equation from the measured and calibrated spot probe reflection. As the data show, there is a significant amount of frequency ripple across the 4 to 20 GHz frequency band which is an artifact of the specimen edge diffraction. Also shown on this plot are data from a larger 6" square specimen measured by a laboratory focused beam system so that there is less edge diffraction error. While the spot probe measurements agree with the focused beam data, there is still a desire to get better accuracy and reduce the effects from the edge diffraction ripple.

Since the measurement technique here acquires data over a wide bandwidth, there is an opportunity for taking advantage of that bandwidth to improve the inversion algorithm. Conceptually, the wide frequency range could be leveraged to "average" or smooth out the measured result. This idea leads to a model-based inversion algorithm, the results of which are also shown in Figure 2.

The idea of a model-based inversion is to apply an analytical model to fit to the measured S_{11} data, which ensures the inverted result is constrained to be a physically valid solution. A well-known model for describing dielectric behavior of condensed matter is the Debye model,

$$\varepsilon = \varepsilon_\infty + \frac{\varepsilon_{DC}-\varepsilon_\infty}{1+i\omega\tau} - \frac{i\sigma}{\omega\varepsilon_0} \qquad (3)$$

In this equation, ε_{DC} is the low frequency permittivity, ε_∞ is the high frequency permittivity, and τ is the damping frequency. This version of the Debye model also includes an additional term that is related to low frequency conductivity, σ. Thus, there are four different parameters used to fit this model to the measured S_{11} data.

To apply the Debye model inversion, the algorithm starts with an estimate of the fit parameters obtained from the frequency-by-frequency inversion. Initial guess values for the low and high frequency permittivity parameters are chosen to bracket the mean permittivity from the frequency-based inversion. The starting point for the damping frequency is chosen to be in measurement band and a small value is chosen for the starting point for conductivity. At this point a standard Nelder-Mead iterative solver is used to optimize the fit between an estimated S_{11} from the Debye model and the measured S_{11} data.

Since time-domain gating is used to filter the measured data it is also applied to the fitted model. This is a subtle but important aspect to the inversion algorithm because gating is known to induce systematic errors at the band edges, particularly with non-symmetric time-domain signals. Using the same time domain gate on both the measured data and the model it is being compared to ensures that gating does not add these errors to the dielectric inversion.

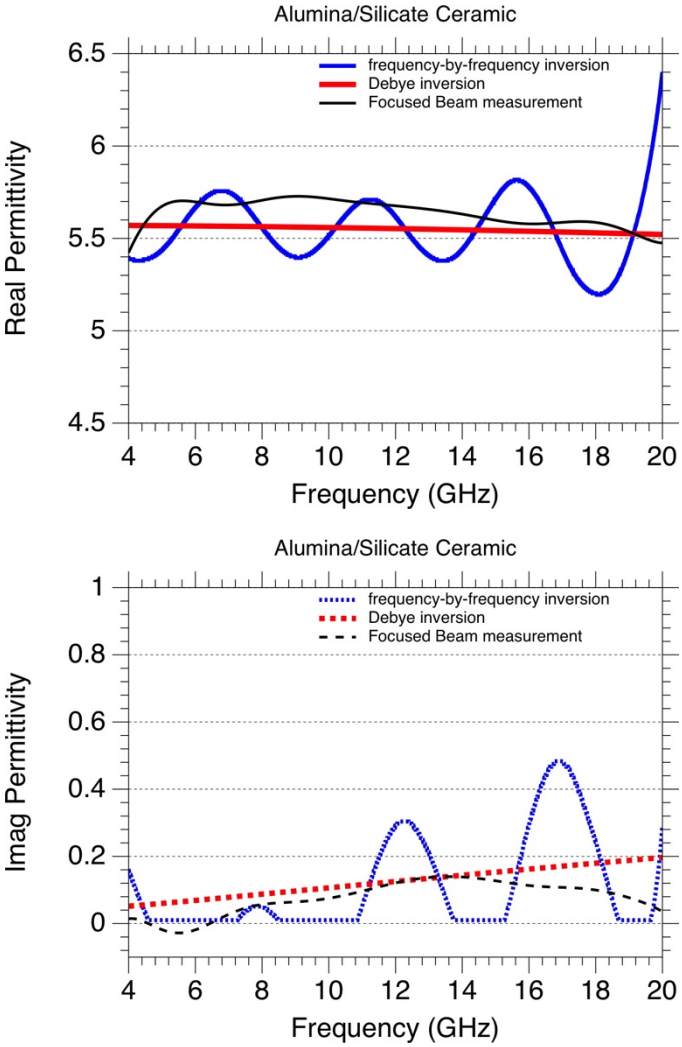

Figure 2 Measured and inverted dielectric permittivity for an Alumina/Silicate Ceramic specimen (top = real, bottom = imaginary).

Example results of this Debye based inversion can be seen in Figure 2. Compared to the frequency-by-frequency inversion in blue, the red Debye inversion curves have eliminated the ripple effect from the anomalous edge diffraction, while still showing agreement with the frequency-by-frequency trends. In this ceramic specimen, a small amount of frequency dispersion is evident – the real permittivity decreases from almost 5.6 at 4 GHz to just above 5.5 at 20 GHz. Corresponding to this change in the real part, the imaginary permittivity shows a small but not insignificant amount of loss across the measurement frequency band. In the frequency-by-frequency inversion results, these trends are difficult to discern because of the effects of diffraction.

In comparison to the laboratory focused beam data shown on the same plots (thin black lines in Figure 2), the Debye inversion shows similar but not exactly the same behavior. One reason for these differences is that the focused beam measurement was made on a different specimen of alumina/silicate material. The exact pedigree of the two measured specimens is not known, so

there could be material differences between the two. Additionally, there are measurement uncertainties associated with both the focused beam technique and with the spot probe technique which are likely responsible for some of the differences.

It is also possible that the Debye equation employed in the model-based inversion does not exactly describe the behavior of the material under test. It is a simplified model and for some materials the frequency dependence is more accurately described with a distribution of Debye relaxation terms. In this case the model would have to be fit to an infinite series, with each term parameterized by a set of variables equivalent to ε_{DC}, ε_{∞}, and τ. While a distribution of Debye terms could potentially improve the accuracy of the fitted frequency dispersion, it adds more variables to the inversion. Searching for the best fit with more variables requires more computation time for the algorithm and additional complexity that could lead to convergence problems. Thus, the choice of model for fitting to the data is a pragmatic one that is focused on using a model that is 'good enough' for the measurement uncertainty of the method while avoiding unnecessary complexity.

IV. Specimen Measurements

With the fixturing and methods described above, a series of measurements were made on core slabs from both conventional (sandstone, limestone) and unconventional rocks (shale). These measurements demonstrate the ability of this method to obtain real and imaginary dielectric permittivity for specimens of interest to the drilling community. Combined with additional knowledge from other diagnostic measurements, wide-band dielectric properties can aid in diagnosing the constituent properties and condition of otherwise unknown material specimens.

A slab of a Mancos shale was measured. The slab was cut on a 1/3 – 2/3 basis. While the 2/3 slab, being a thicker sample, was a better specimen for this method, it exhibited several fractures produced during handling. Thus the 1/3 slab was measured instead because of its physical integrity. However, the maximum thickness of this sample is about 1.3 inches, thus a smaller time gate of 0.32 ns was chosen to minimize reflections from the backside of the slab.

Shales are a mixture of organic material such as kerogen and bitumen, as well as clays and carbonates. In addition to the conductive clays, many shales are also composed of conductive minerals such as pyrite and marcasite. Shales with high clay content exhibit a polar behavior that increases with water content. Thus, they are well described by Debye relaxation and a good candidate for the Debye inversion in this effort.

The measured Mancos shale slab came from an outcrop and has a high clay to organic content [5]. Clays tend to exhibit significant conductivity due to water content. Even when water is removed, clays retain some conductivity due to their cation-exchange capacity. Figure 3 shows the inverted results for the complex permittivity of the Mancos shale sample. The real part is consistent with values shown in the literature [6, 7]. Also, it easy to see the small frequency dispersive behavior at frequencies below 10 GHz, which has also been observed in transmission line measurements for high clay content shales in the laboratory. However, this Mancos shale specimen exhibits higher than expected losses [6], which are typically between 0.5 and 0.1. This additional loss may indicate the presence of higher salinity water in the clays (if any), highly charged clays or the presence of conductive minerals. A full geochemical analysis needs to be done to establish a correlation with these measurements.

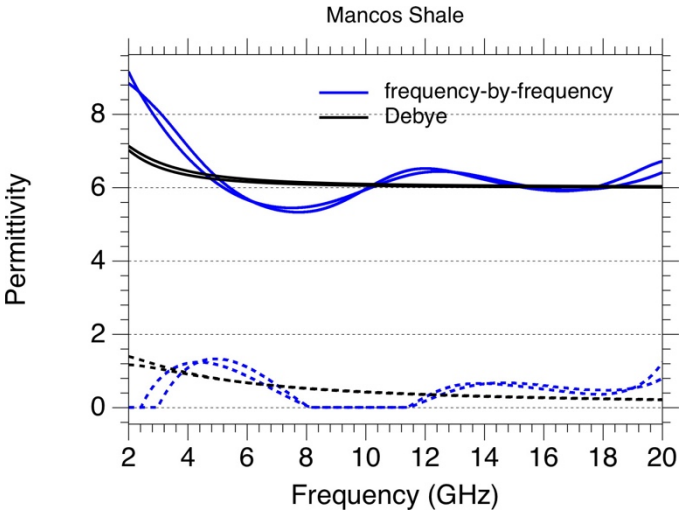

Figure 3 Real (solid lines) and imaginary (dashed lines) permittivity of Mancos Shale using both inversion algorithms.

Measurements made of conventional rocks included two limestone samples and two sandstone samples. The limestone slabs were Indiana and Edwards white. The respective sandstone slabs were Berea and Torrey Buff. These conventional rock slabs were dry and the thicker, 2/3 slab was measured. Some general physical properties of the measured slabs from the core provider are given in Table I.

TABLE I. Conventional Rock Slab Physical Properties.

Rock	Porosity	Permeability
Indiana Limestone	12%-14%	2mD-4mD
Edwards White Limestone	16%-19%	1.5mD-3mD
Berea Sandstone	18%-21%	80mD-120mD
Torrey Buff	13%-17%	0.4mD-3mD

Figure 4 shows the inverted dielectric properties of the four conventional slabs. The near frequency-independent behavior of the real part (values between 4 and 7) of the complex permittivity agree well with both published results [7, 8] and in-house resonant sandstone measurements. There is an obvious, and expected, influence of porosity in dry rocks: More porous rocks will have a higher air content which brings the real relative permittivity down. As shown in Table I, these materials have air content in the range of 12 to 21 percent. This trend is observed for both limestone and sandstone samples. Moreover, the values obtained for both types of rock lie within previously reported intervals in the literature [7, 8].

The losses for all four conventional dry rock samples are, as expected, in the range below 5×10^{-2}. Such low losses are due to the lack of water in the pore space and the inherent low loss

nature of the main components of limestone (calcium carbonate) and sandstone (quartz). Such low imaginary values are below the measurement uncertainty of the spot probe method. However, the intent of the spot probe is to characterize slab specimens freshly obtained from a well. These specimens more often than not will have a small fraction of water present in the rock pore space, which is easily detected by this method.

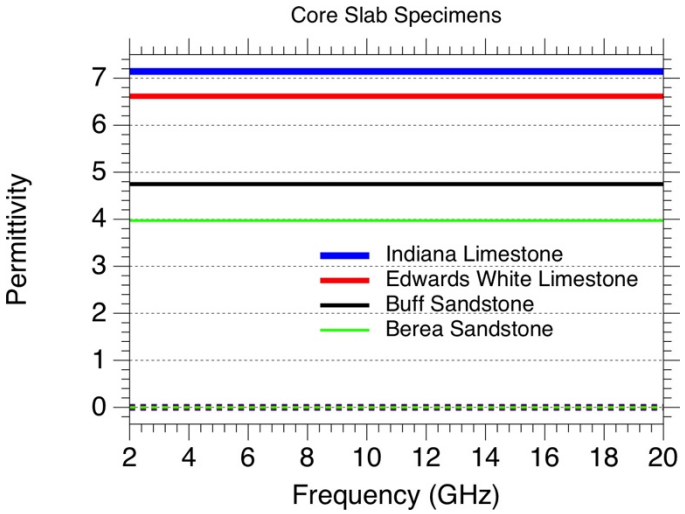

Figure 4 Summary of measured permittivity for conventional, low-loss rock specimens extracted using the Debye inversion method. Relative real (solid lines) and relative imaginary (dashed lines) permittivity.

V. Conclusion

This paper presents a new method for determining wide-band dielectric permittivity of core-slab specimens obtained from wells. It utilizes a recently developed spot probe technology for illuminating a specimen. A key feature of the method is that it assumes an electrically thick specimen and uses only the reflection from the front surface to determine dielectric properties. Time domain gating is used to screen out the reflections from the back side of the specimen, which is not planar. Thus, semi-cylindrical specimens, which are typical of core-slab geometries obtained in the drilling industry, can be characterized. The relatively small diameter of the core-slab specimens results in frequency ripple induced by edge diffraction. Therefore, a model-based inversion was adopted to minimize errors from this effect. A Debye relaxation model with an additional conductivity term was used for this inversion and is fit to the measured data to obtain dielectric properties.

Finally, this new measurement method is demonstrated on several conventional and unconventional rock specimens. Both low-loss and lossy rocks were measured, showing the ability of this method to measure a range of materials. In specimens freshly obtained from a well, significant water content is common, and exhibits increased dielectric loss. The data shown here prove the feasibility of the method for measuring this loss and show its usefulness for characterizing fresh core specimens. The probe and fixturing is very compact and portable, especially if combined with a compact 1-port microwave network analyzer. This makes it suitable for use in a field laboratory. Ultimately this work will help with the design of a tool to go down a well where characterization of water content and other rock properties is desired.

Acknowledgement

Author J.O. Alvarez want to thank Susan Agar, Dawn Jobe and Lauren Stout at the Geology Technology Team, Aramco Services Company: Aramco Research Center – Houston, for providing core the slabs for measurements.

References

[1] C. McPhee, J. Reed and I. Zubizarreta, Core Analysis: A Best Practice Guide, 1st ed., vol. 64. Elsevier: Developments in Petroleum Science, 2015, Chapter 1.

[2] F. Jahn, M. Cook and M. Graham, Hydrocarbon Exploration and Production, 2nd ed., vol. 55. Elsevier: Developments in Petroleum Science, 2008, pp. 141-145.

[3] J. Musil, F. Zacek, A. Burger, J. Karlovsky, "New Microwave System to Determine the Complex Permittivity of Small Dielectric and Semiconducting Samples," 4th European Microwave Conference, 66-70, 1974.

[4] J.W. Schultz, J.G. Maloney, K.Cummings, R.B. Schultz, "A Comparison of Material Measurement Accuracy of RF Spot Probes to a Lens-Based Focused Beam System", AMTA Proceedings, 2014.

[5] R.F. Broadhead, "The Upper Mancos Shale in the San Juan Basin: Three Oil and Gas Plays, Conventional and Unconventional: Update", AAPG Annual Convention & Exhibition Proceedings, 2018.

[6] J.O. Alvarez and F.L. Peñaranda-Foix, "Multi-Frequency Microwave Resonance Cavity for Nondestructive Core Plug Measurements", IEEE Int. Geoscience and Remote Sens. Symp. (IGARSS) Proceedings, 2018.

[7] D.J. Daniels, Ground Penetrating Radar, 2nd Edition, vol. 15. IET Radar, Sonar, Navigation and Avionics Series, 2007, chapter 4.

[8] F. T. Ullaby, T. H. Bengal, M. C. Dobson, J. R. East, J. B. Garvin, and D. L. Evans "Microwave Dielectric Properties of Dry Rocks" IEEE Trans. Geosci. Remote Sens., vol. 28, no. 1, pp. 325-34, May 1990.